Analysis of Twisted Nematic Gratings Based on Azo-Dye-Doped Liquid Crystals



Allegheny College

Brian Chiang
Department of Chemistry
Department of Physics
April 2010

Analysis of Twisted Nematic Gratings Based on Azo-Dye-Doped Liquid Crystals

Brian Chiang

Comprehensive Senior Project

Submitted to the Allegheny College Departments of Chemistry and Physics to partially fulfill the requirements for the degree of Bachelor of Science.



Advisor: Dr. David Statman

Second Reader: Dr. Shaun Murphree

Second Reader: Dr. Daniel Willey

I hereby recognize and pledge to fulfill my responsibilities, as defined in the Honor Code, and to maintain the integrity of both myself and the College Community as a whole.

Pledge:_____

Brian Chiang

Abstract

Twisted nematic gratings were fabricated by a polarization holographic approach, on azo-dye-doped liquid crystal cells. By varying the conditions under which they are fabricated, (surface coatings, dyes, angle of holographic writing) it can be observed how each factor affects the grating efficiency and Stokes Parameters of diffracted beams. Diffraction efficiencies were as high as 2.5% for samples doped with Methyl Red, and were below 1% for samples doped with Disperse Orange 3. The polarization states of the zeroth-order and first-order diffracted beams are perpendicular to each other. Gratings were not fully erasable when irradiated with linearly polarized light. Disperse Red 13 was shown to be incapable of forming gratings, revealing azo-dye-induced director reorientation to play a major role. No conclusions could be drawn between the use of polyimide and polyvinyl alcohol films.

Table of Contents

1. Introduction 1

2. Theory..... 2

3. Experiment..... 12

4. Results and Discussion..... 16

5. Conclusions..... 22

6. References..... 23

7. Appendix A..... 25

8. Appendix B..... 29

9. Appendix C..... 31

Introduction

The liquid crystal phase was first discovered in 1888 when Austrian chemist Friedrich Reinitzer tried determining the melting point of a derivative of cholesterol. He was surprised to find that at 145.5°C, the solid crystal melted into a cloudy liquid and at 178.5°C, the substance became a clear liquid. At first, he suspected this to be a sign of impurities within the substance, but after further purification, the substance provided the same behavior. With the help of German physicist Otto Lehmann, an expert in crystal optics, they were able to conclude that the cloudy phase had a unique order similar to that of solid crystals and that the clear phase had the same characteristic disorder of common isotropic liquids[1].

Liquid crystals have found tremendous usefulness in optics and most notably in display applications. Although this lesser known phase of matter is not often considered for common substances, liquid crystals are not very rare, and can be found in nature, soap solutions, and in human blood[2].

Liquid crystals have been adopted widely for fabricating various gratings due to their potential to act as switchable diffractive optical elements. Twisted nematic gratings are expected to function as polarization gratings; they periodically modulate the polarization of light as it passes through, producing new polarization states in the diffracted beams. The diffracted beams can then be controlled using a rotating analyzer. In an effort to understand what determines the characteristics of these gratings, a holographic approach on the basis of the laser-induced adsorption of azo dyes by a polymer-coated glass substrate should help illuminate the roles of the conditions upon fabrication.

Theory

Calamitic liquid crystals are a class of rod-shaped molecules, meaning one axis is significantly longer than the other two. The nematic phase possesses orientational order, with respect to the lengthwise axis of the molecules, but no positional order, (i.e. molecules are not bound to specific layers or rigid lattices) thus, they possess properties of both liquids and crystals. The liquid crystal mixture used in our experiment, E7 (Licristal), is a mix of structurally similar, calamitic, nematic phase liquid crystals. The advantage of using a liquid crystal mixture is that the nematic phase has a broader temperature range than that of its pure components.

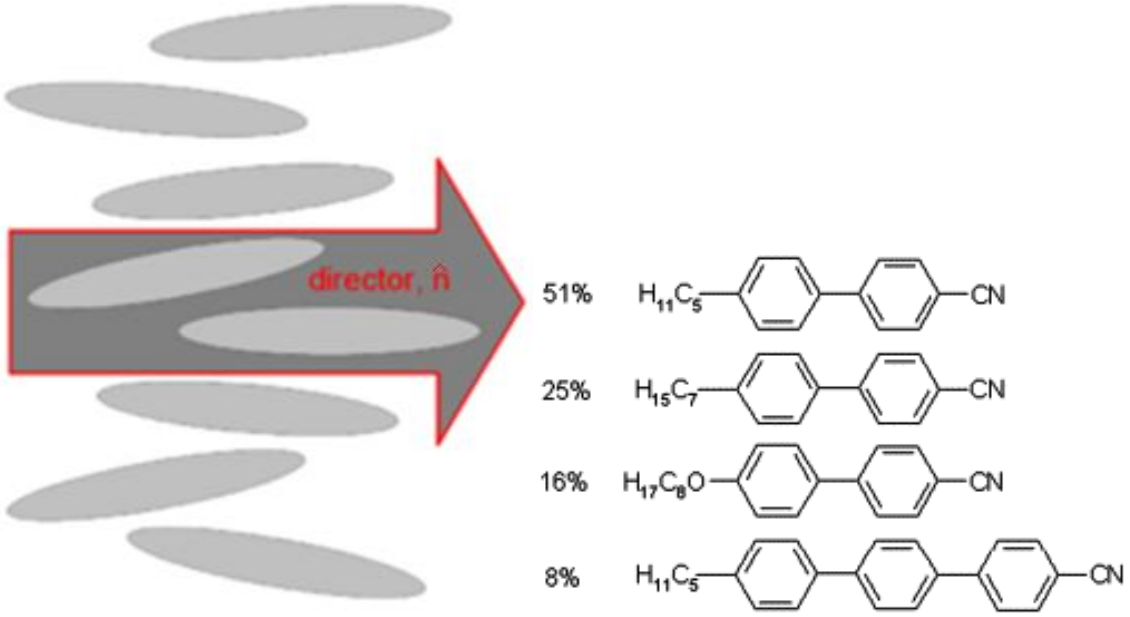

Figure 1: *Left*: The average of the lengthwise direction is represented by the director $\hat{n}$. *Right:* The components of E7, a liquid crystal mixture used in displays because of the broad temperature range of its nematic phase. The rigid phenyl rings maintain the molecules' oblong geometry while allowing electron density to flow towards the cyano groups, which are electron withdrawing to enhance molecular polarizability. The presence of an electron donating group on the opposite end, such as the component second from the bottom, serve to provide further enhancement.

The liquid crystal order is specified by the order parameter

$$S = \langle P_2(cos\theta) \rangle = \langle \frac{3}{2} cos^2\theta - \frac{1}{2} \rangle \quad (1)$$

Where P_2 is the second Legendre polynomial and θ is the angle each molecule makes with the director. The brackets denote an average over many molecules or an average of one molecule over time.

Legendre polynomials provide handy distribution functions f(θ)dθ. The second Legendre polynomial is commonly used because the odd Legendre polynomials average to zero, and higher order Legendre polynomials are more difficult to measure. When S = 1, the liquid crystals have complete orientational order. When S = 0, the molecules are completely disorganized. In a typical liquid crystal, S decreases as the temperature is raised, taking on values between 0.3 and 0.8. The order parameter can be measured by means of measurements of diamagnetism, birefringence, nuclear magnetic resonance, and Raman scattering[2].

When an electric field $\vec{E}$ is introduced, liquid crystals gain induced electric dipole moments, as electron density is pulled to one end of the molecule. The electric field then generates a torque on the dipole to reorient $\hat{n}$ along $\vec{E}$. The cyano groups common to all components of E7, (Figure 1) serve to enhance the polarizability by withdrawing electrons from the phenyl groups to delocalize charge. The presence of an electron donating group on the opposite end serves to provide further enhancement, by directing electron density in the direction of the electron withdrawing group.

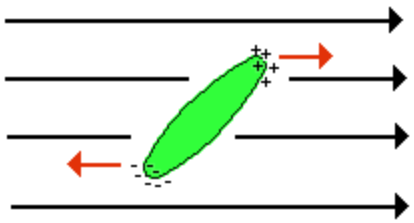

Figure 2: An electric field separates the charges on a liquid crystal molecule[17].

The induced dipole moment per unit volume is given by

$$\vec{P} = \varepsilon_0 \chi_e (\hat{n} \cdot \vec{E}) \hat{n} \qquad (2)$$

Where ε_0 is the permittivity of free space and χ_e is the electric susceptibility.

Hence the torque per unit volume is then given by

$$\vec{\Gamma} = \vec{P} \times \vec{E} \qquad (3)$$

Liquid crystals do not undergo reorientation without resistance. The inner surfaces of a liquid crystal cell exert some hindrance to reorientation, termed "anchoring" (See Appendix A for a description of liquid crystal cells.). An appropriate selection of polymer coating on the inner surfaces determines the level of anchoring, and a number of pretreatment methods can be used to set a preferred orientation direction with the polymer.

The Freédericksz Transition is when the electric field is strong enough to supply the minimum required energy for reorientation. If the electric field is too weak, the molecules will not move. Distortions from the equilibrium state of the director are described by three main classes: splay, twist, and bend.

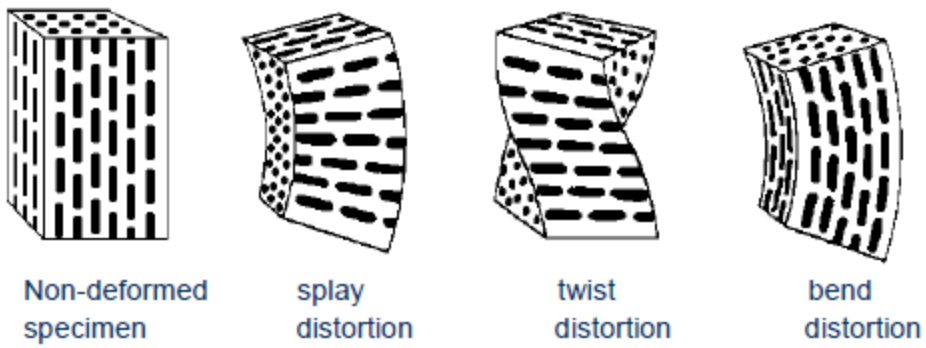

Figure 3: Classifications of distortion in the director field[3].

The free energy density used to describe the liquid crystal's opposition to distortion is given by

$$F_v = \frac{1}{2}K_1[\nabla \cdot \hat{n}]^2 + \frac{1}{2}K_2[\hat{n} \cdot (\nabla \times \hat{n})]^2 + \frac{1}{2}K_3|\hat{n} \times (\nabla \times \hat{n})|^2 \qquad (4)$$

Where K1 is the splay distortion constant, K2 is the twist distortion constant, and K3 is the bend distortion constant. These three constants are analogous to the spring constant and describe the liquid crystal molecules' attachment to distortions of the director. Typical values of these constants are on the order of 10^{-11} Newtons, with K_3 being two to three times larger than K_1 and K_2. These constants are greater when the order parameter is greater[2].

Since the free energy density is higher in the presence of distortions, the liquid crystal will want to spontaneously return to its undistorted state. For molecules within the bulk of the cell where anchoring effects from the surface are negligible, reorientation occurs quickly. For molecules at the surface which feel the full strength of surface anchoring, reorientation occurs slowly. Even though molecules within the bulk represent the large majority of the liquid crystal, they will go back to their initial position unless molecules at the surfaces are rotated as well. Rotation of liquid crystal at the surface is known as "gliding". Gliding is a slow process and results in a semi-permanent change in the "easy axis" of the sample. It is along the easy axis that the anchoring interaction between the liquid crystal and the polymer is minimized, which represents the preferred direction of $\hat{n}$.

To get a sense for the order of magnitude required for the Freédericksz Transition, consider that the threshold electric field for a twist deformation E_t, which would be the main consideration for forming a twisted nematic grating, can be expressed as

$$E_t = \frac{\pi}{d}\sqrt{\frac{K_2}{\varepsilon_0 \Delta \chi_e}} \quad (5)$$

Where d is the thickness of the cell, ε_0 is the permittivity of free space, and χ_e is the electric susceptibility[2].

For a typical nematic liquid crystal cell of a thickness of 25 microns, $E_t \approx 10^3 \frac{N}{C}$. This is quite a large field, but it would be helpful to approximate the intensity of a laser which is producing this field during the holographic inscription process, using the relationship

$$I = \frac{c n_a \varepsilon_0}{2} |E|^2 \quad (6)$$

Where c is the speed of light and n_a is the mean refractive index of E7 at 488 nm (~1.6).

This relationship arises from the fact that light is composed of oscillating electromagnetic waves, containing two mutually orthogonal polarization states, pertaining to the oscillating electric and magnetic fields. Since the torque exerted by the magnetic field on an electron averages to zero, one typically considers the polarization of light solely in terms of the direction which the electric field oscillates. This allows for one to control the direction for reorientation, by manipulating the polarization of light with optical elements.

The calculated laser beam intensity is on the order of $10^9 \frac{W}{m^2}$, which is far too intense for many of the optical elements to handle. In order to lower the energy required for the Freédericksz Transition, we employ the use of azo-dyes in very small amounts (~0.5% - 1% w/w). The azo-group is a pair of double-bonded nitrogens that lie at the core of our azo-dyes.

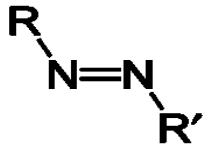

Figure 4: The azo functional group. In its equilibrium state, the R groups are in the trans state, as shown.

At equilibrium, azo-groups are in the stable trans state, and the double bond does not allow rotation to the meta-stable cis state. Azo-groups undergo photoisomerization when the wavelength of the laser is within the absorption band of the azo-dye. Electrons in the azo-dye absorb photons from the laser to reach an excited state in which the double bond is disrupted, where the azo-dye can thermally relax into the cis or trans state. While the azo-dyes are in the trans state, they are also rod-shaped as the liquid crystals are, and are scattered within the bulk. When the azo-dyes are excited to the cis state, they are more compact, but less ordered. Since this cis state is not very stable, it thermally relaxes to the trans state after a short time. With a change in conformation comes a change in the dipole moment of the molecule, and one often chooses an azo-dye with an increased dipole moment in the cis form, so that the enhanced dipole-dipole interactions between the dye and the surface are activated by the beam of absorbed light. While in the cis form, the enhanced dipole-dipole interactions cause the dye molecules to be drawn to and adsorbed onto the surfaces of the cell, before relaxing to the trans form[19].

It turns out that the final orientation of the dye molecules is perpendicular to the polarization of the light it absorbed. This is because the chance of absorbing a photon is proportional to the cross-sectional area of the molecule from the standpoint of incoming light. Therefore, maximum absorption occurs when trans isomers are parallel to the polarization of light, and minimum absorption occurs when trans isomers are perpendicular to the polarization of light; azo-dye molecules will continually absorb photons and relax in some random orientation until they are perpendicular to the polarization of light.

As a result of azo-dye molecules being adsorbed onto the surfaces of the cell with an orientation imposed by a laser, a competition between the orientation set by the polymer coating and the orientation set by the azo-dye occurs. Once enough of the azo-dye has adsorbed onto a surface, it will have effectively overwritten the orientation set by the polymer coating, and the liquid crystal molecules align themselves in the same orientation as the azo-dye molecules. This mechanism allows for the formation of the twisted nematic grating, but a twisted nematic grating requires one surface to impose an orientation different from that of the other, so that the director twists from one surface to the other.

Diffraction gratings that operate by periodically modulating the polarization of light passing through them are generally classified as "polarization gratings"[4]. We can generate such a grating using left-circularly and right-circularly polarized beams which interfere to write a hologram in the substrate. As discussed in Appendix C, the interference of these beams will generate an interference pattern of linear polarization. Since the relative distances between the two beams will differ for different observation points within the region of overlap, the phase difference will also differ, presenting an array of different linear polarizations as pictured[5]:

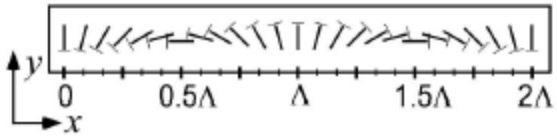

Figure 5: The pattern generated by the interference of right-circularly and left-circularly polarized light.

One should also expect, from Beer's Law, that the light transmitted through the sample is decreasing as it passes through:

$$T = \frac{I}{I_0} = 10^{-\varepsilon c l} \qquad (7)$$

Where T is the transmittance, ε is the molar absorptivity, c is the concentration of absorbing species in the sample, l is the distance the light travels through the sample, I is the intensity after traveling through l, and I_0 is intensity of incident light.

Approximating the ε for Methyl Red to be around 2.3 x 10^4 M^{-1} cm^{-1}, the density of E7 to be close to 2 kg/L, and the molar mass of Methyl Red to be around 0.27 kg/mol, we find that for a sample doped 0.5% w/w with Methyl Red, about 90% of the light is lost within the first 10 microns of the sample, assuming the light is not so intense that it saturates the sample. This means that we would have significantly higher dye adsorption on one surface than the other, meaning one face of the cell takes on the interference pattern shown in Fig. 5, while the other remains in its original orientation. The result is:

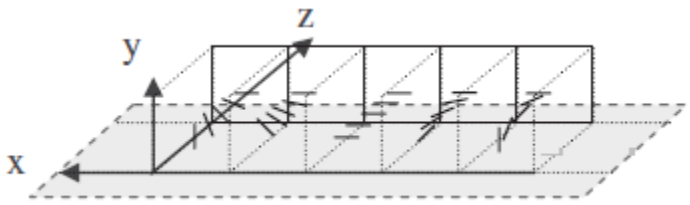

Figure 6: The interference pattern from the right-circularly and left-circularly polarized beams only shows on one face of the cell. The liquid crystal within the bulk gradually rotates to the orientation retained on the opposite face of the cell.

A hologram is an interference pattern containing both the amplitude and phase scattered by an original light wave. The amplitude and phase is stored in the periodic array of the liquid crystal, which makes it a volume hologram. The periodic array of a volume hologram scatters light according to Bragg's Law, as it can be likened to the periodic lattice of a solid crystal which scatters X-rays by Bragg's Law[6].

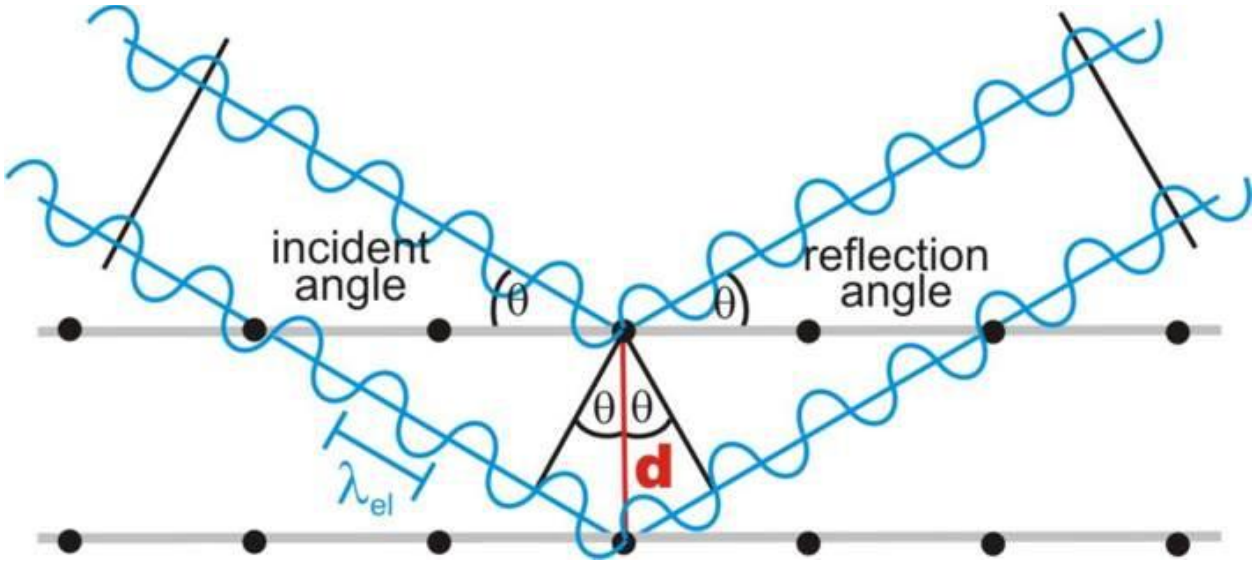

Figure 7: Bragg's Law of Diffraction. The condition for constructive interference of waves is $m\lambda = 2d\sin\Theta$[18].

Thus, the angle of the diffracted probe beams can be predicted from the angle of the write beams by the relation:

$$\frac{\theta_1}{\theta_2} = \frac{\sin^{-1}(m\lambda_1/2d)}{\sin^{-1}(m\lambda_2/2d)} \qquad (8)$$

Where θ_1/θ_2 is the proportion between the angle of the write beams and the angle between the zeroth and first-order diffracted beams, m is the order, and λ_1 & λ_2 are the wavelengths of the write beams and probe beam.

For write beams at 488 nm and a probe beam at 633 nm, the angle between the zeroth and first-order diffracted beams is about 1.3 times that of the writing angle. With this, we have a way of predicting the path of the diffracted beams to be analyzed, before they have formed.

Experiment

The preparation of sample cells is described in Appendix A. The following samples were prepared:

	Doped with MR	Doped with DR13	Doped with DO3
Coated with PVA	X	X	X
Coated with PI	X	X	X

Table 1: A table of the types of samples prepared.

All samples had one surface coated with PEMA and all samples used liquid crystal mixture E7. It was originally planned to make several sets of different thicknesses, but flaws in the sample preparation procedure have resulted in non-uniform thickness. A discussion of these flaws is in Appendix A.

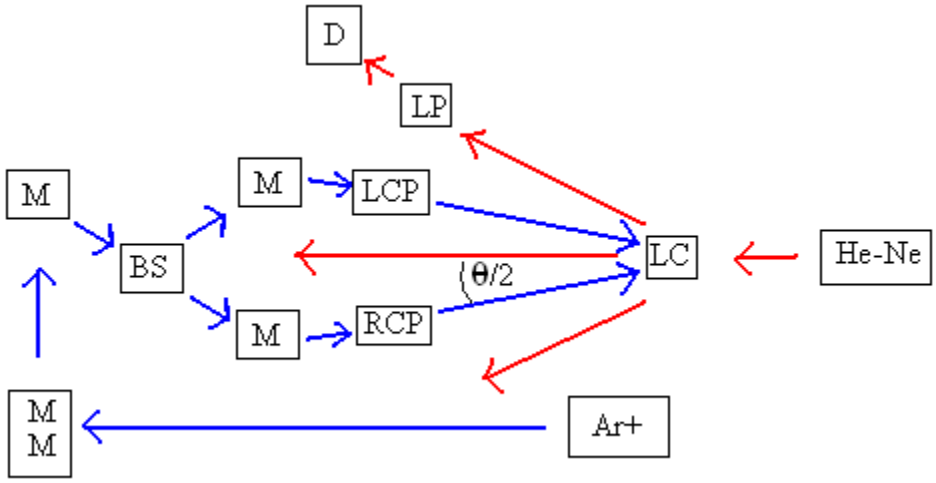

Figure 8: Setup for holographic writing. The blue arrows describe the path of the pump beams. The red arrows describe the path of the probe beam. Ar^+ - Argon ion laser, M - Mirror, LP - Linear polarizer, LCP - Left circular polarizer, RCP - Right circular polarizer, BS - Beam splitter, LC - Sample cell, He-Ne - Helium/Neon laser, D - Detector.

First, we can consider the path of the pump beams which write the hologram. Light emitted from the pump laser is horizontally polarized. This light is directed towards the dual mirror apparatus, which contains two mirrors angled 45° to the incident beam. The beam is then directed towards another "mirror" (This "mirror" was actually a beam splitter with a Reflection/Transmission ratio of 70/30, which functioned as a mirror for my purpose. The transmitted beam was used by another student, and the reflected beam was used by me.) which sends it at a 45° angle to a beam splitter with a Reflection/Transmission ratio of 50/50. The specific polarization of the beam is not too important at this point. Once split, the beams continued until they reached the LCP and RCP. The RCP and LCP are lenses from Real-D, the very same which are now used for viewing movies in 3-D. They function as a linear polarizer set 45° to a quarter-wave plate, to produce the desired circular polarization[7]. The lenses are arranged such that the incident beam goes through the linearly polarizing side first. The two oppositely circular beams then go on to interfere on the LC.

Coherence of beams

For an ideal coherence of interfering beams, one would want the path lengths of the beams from the beam splitter to the interfering region to be exactly the same. Not only that, but the beams must overlap completely and perfectly. Since the optical elements and their alignment are likely to be less than perfect using even the best technique, the next best thing would be to reason that the path length differences of my setup are negligible. It turns out that path length differences are actually negligible as long as they are shorter than a coherence length, which depends on the range of frequencies of the light by the following relation[5]:

$$l_t = \frac{c}{\Delta \upsilon} \qquad \text{Eqn. 9}$$

Where l_t is the coherence length, c is the speed of light, and $\Delta\upsilon$ is the range of frequencies.

For a monochromatic laser, the coherence length can range between tens of centimeters to tens of kilometers, depending on the laser. For the use of holography, an etalon is normally employed for an Ar^+ laser, to plentifully extend the coherence length. A white light source typically has a coherence length around 1 μm. As long as my error is on the order of centimeters, there should be no problem.

The significance of the angle is that it controls the grating spacing. The grating spacing is given by,

$$\Lambda = \frac{\lambda}{2n_{ave}\sin(\theta/2)} \qquad (10)$$

Where λ is the wavelength of the pump beams (488 nm), n_{ave} is the mean refractive index of the liquid crystal [$n_{ave} = (2n_o + n_e)/3 \sim 1.6$], and θ is the angle of intersection of the write beams.

The probe beam is diffracted from the grating while the hologram is being written to make dynamic measurements of the diffraction efficiency. The diffraction efficiency is given by the proportion of the intensity of the first-order diffracted beam with that of the incident light under a parallel polarizer. The zeroth and first order beams are drawn in Fig. 8. A linear polarizer and detector are shown measuring the Stokes Parameters (Appendix C) of the diffracted beams. Gratings can also be examined under a cross-polarized OPM to qualitatively examine the contrast between fringes and to measure the separation distance between fringes to make sure the values agree with (10).

The optical table was floated during the writing process to prevent vibrations from disrupting the hologram. The diameter of the interference region was about 5 mm. The diameter of the probe beam was about 2 mm. The power of the write beams were about 18 mW/cm^2. The incident light from the probe was 80.9 mW/cm^2. A chopper and a lock-in amplifier were used to filter out stray light sources other than the probe. The writing process and data gathering were done at room temperature. Grating spacing was measured using a cross-polarized microscope.

Results and Discussion

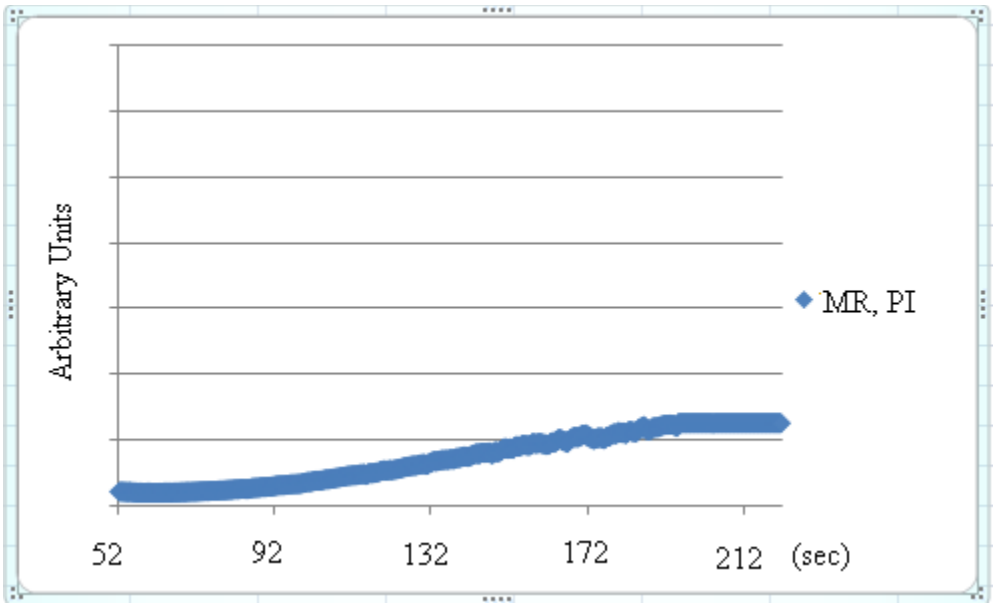

Figure 9: Diffraction efficiency of a 10 micron grating, written on a cell coated with PI and PEMA, filled with E7 doped with 0.5% (w/w) Methyl Red, ~60 microns thick. The diffraction efficiency appears to reach its maximum of 2.5% at around 195 seconds. Other gratings were written at comparable speeds.

	First Order	
PI	MR	DO3
S_0	1	1
S_1	-0.66667	-0.91736
S_2	-0.34444	0.046832
S_3	0	0.393939
DE	2.50%	0.50%

	Zero Order	
PI	MR	DO3
S_0	1	1
S_1	-0.07057	-0.91416
S_2	-0.09057	-0.24893
S_3	-0.15094	-0.78541

	First Order	
PVA	DO3	
S_0	1	
S_1	-0.85027	
S_2	-0.06952	
S_3	0.272727	
DE	0.03%	

	Zero Order	
PVA	DO3	
S_0	1	
S_1	-0.92746	
S_2	-0.2339	
S_3	-0.72881	

Table 2: Tabulated normalized Stokes Parameters and diffraction efficiencies (DE) for the first and zeroth order diffracted beams, for gratings written to be of 10 microns.

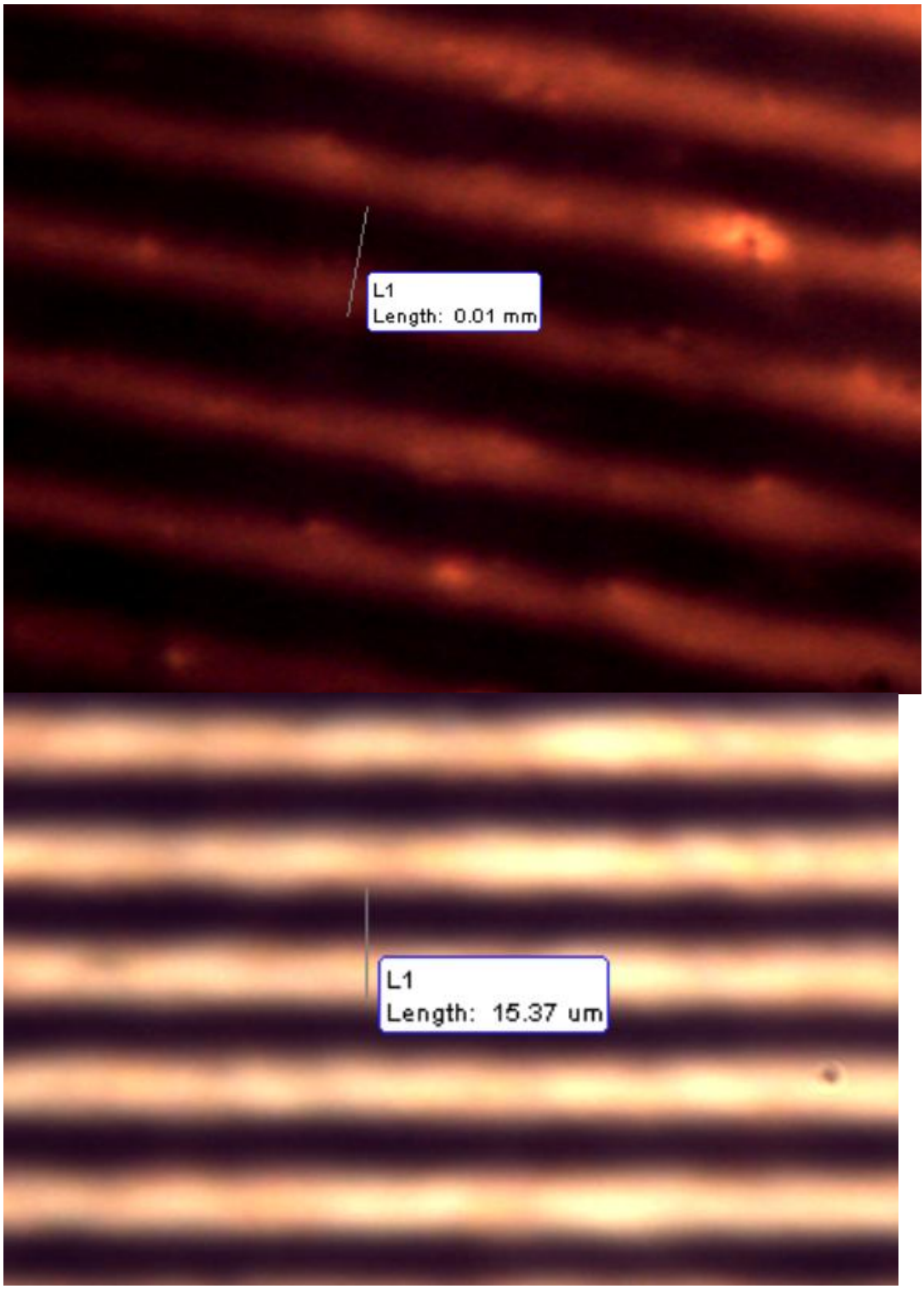

Figure 10: Top: ~10 micron grating, written on a cell coated with PI and doped with MR. Bottom: ~15 micron grating, written on a cell coated with PVA and doped with MR. Both were written at the same angle and both are about 60 microns thick.

At a glance, it seems some data is missing from Figure 9 and Table 2. Gratings with DR13 could not be formed because it was realized that DR13 is not a suitable azo-dye for director reorientation experiments[8]. It would seem that the relaxation time of the cis isomer is too short (about two orders of magnitude faster than for DO3) because of the instability of the cis isomer[9-10]. Since it relaxes so quickly, the cis fraction of isomers is quite small at any given time, so there would not be many cis isomers to be adsorbed onto the polymer. Even long irradiation times of up to an hour, on both types of samples doped with DR13, produced no sign of grating formation.

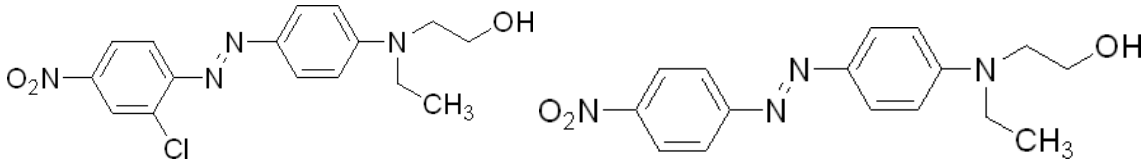

Figure 10: Disperse Red 13 (left) and Disperse Red 1 (right). DR1 has been shown to be suitable for director reorientation experiments, but DR13 is not. The difference is the Chlorine attached to DR13, which has an electrostatic repulsion with the phenyl ring on the other side of the azo group, when it is in the cis state.

Additionally, it would seem that in trying to erase early gratings so I could rewrite them for better gratings, I have ruined some samples before I analyzed them. At first, it sounded feasible to erase a grating similarly to how it was written, by shining a beam of light which has been polarized perpendicular to the rubbing direction, which would reorient dye molecules back to the rubbing direction. Surprisingly, even after being irradiated for over an hour, the gratings created with MR remained persistent. Clearly, a substantial fraction of adsorbed dye molecules were not being reoriented by this method.

The layer of adsorbed molecules is actually several layers of dye molecules thick even before a laser is brought in[11]. It is thought that the desorption-reorientation-adsorption process, which is responsible for director reorientation, will not completely erase the previous step because the layers which are closer to the polymer surface are more strongly adsorbed to the point that there is little to no reorientation[12].

After attempting to erase gratings with light, several attempts were made to erase gratings by heating. Heating the gratings past the clearing point of E7 (~64°C) causes a disruption in the orientation of the layer of azo-dye. Several heating and cooling cycles are expected to erase the gratings completely[21], but it was not until I had tried this on several samples before I realized that even trying to heat the sample near the clearing point of E7 was destroying the order on my samples. The reason for this was because the glass transition temperature of PEMA, the polymer common to all of my samples, is actually close to the same temperature as the clearing point of E7, so there is no way to heat above the clearing point without also permanently disrupting the order of my sample from the phase change in PEMA[20].

I had been working under the assumption that the gratings were easily erasable, so when I started to realize my erasing process was not working, I had already ruined several of my gratings without having gathered all the data I wanted, without leaving enough time to make new samples to gather data from. With this limitation, I was unable to get enough data to say anything conclusive about the use of PI versus PVA. Both behave quite similarly and both are used to successfully make Twisted Nematic Gratings[13-15].

This problem only applies in part to the case of the samples doped with Disperse Orange 3. A very peculiar phenomenon occurs, in which the grating forms at a speed comparable to the samples doped with Methyl Red, disappears as soon as the write beams are blocked, then reappears instantly, and stronger when the write beams are reintroduced. These results agree with those seen in similar director reorientation experiments[16]. The key difference in the chemical structures between Methyl Red and Disperse Orange 3 lies in the carboxylic acid group on Methyl Red.

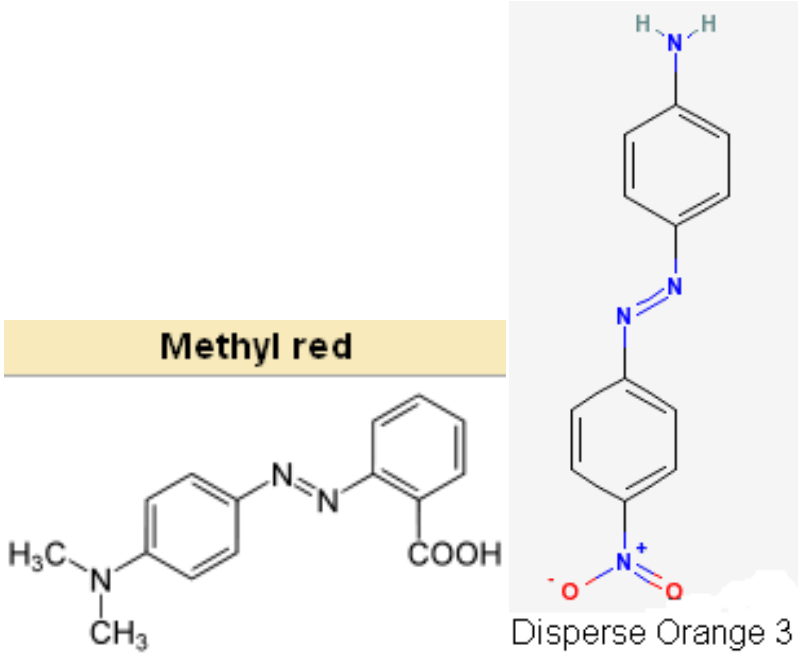

Figure 11: The structures of Methyl Red and Disperse Orange 3.

The carboxylic acid group on MR allows the molecule to lose a proton to take on a much stronger dipole moment than DO3. This would allow superior adsorption onto a surface for MR, in comparison to DO3. Perhaps with a more polar polymer surface, DO3 could have persistent adsorption, but it was not observed for either PI or PVA.

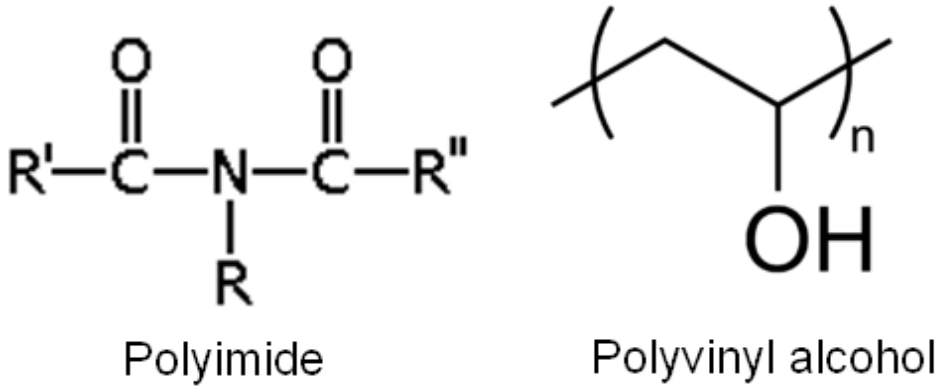

Figure 12: The structures of PI and PVA.

Although DO3's behavior is not well understood, one possibility is that the cis isomers are weakly adsorbed onto the surface while the write beams are on. When the write beams are turned off, the DO3 molecules relax to the trans form and are no longer adsorbed onto the surface, but perhaps stay within a close proximity. This could explain how the grating is reformed so quickly when the beams return.

I only managed to get one measurement of a grating written at a wider angle, resulting in a grating with smaller fringe spacing. On a sample with a PI coating and doped with DO3, I wrote a grating for 5 micron spacing. Since I had written on the grating previously, the grating immediately appeared and had a grating efficiency of 0.135%. Shifting that same grating back to the 10 micron fringe placement produced a higher grating efficiency of 0.167%. One could conclude that wider fringe spacing produces higher grating efficiency, since the fringe spacing represents how gradually the director rotates from fringe to fringe. Writing a smaller fringe spacing means the director must rotate more within a given space, which is energetically unfavorable and more subject to defects.

Conclusions

Twisted Nematic Polarization Gratings were successfully written, using two of the three azo-dyes originally planned. No significant differences were observed between the use of a PI coating versus a PVA coating. Samples doped with DR13 could not produce a grating, as the azo-dye induced director reorientation is a vital sequence of grating formation. Samples doped with DO3 could not produce lasting gratings, because of insufficiently strong dipole-dipole interactions. A priming effect was observed, in which previously written samples doped with DO3 showed an immediate reformation of gratings when reintroduced to the pump beams; possibly indicating a redistribution of azo-dye molecules within the sample. Further investigation with this project is possible, to further explore the roles of different azo-dyes, surface-alignment polymers, and other holographic inscription parameters.

References

[1] *History and Properties of Liquid Crystals*. Nobel Web. 2003.

[2] P.J. Collings and M. Hird. Introduction to liquid Crystals (Taylor & Francis Publishers, Philadelphia, 1997)

[3] Elliot, J. *Modeling of Liquid Crystal Polymer Processing*. University of Cambridge. 2005.

[4] M. J. Escuti & W. M. Jones. *Polarization-Independent Switching with High-Contrast From A Liquid Crystal Polarization Grating*. SID Int. Symp. Dig. Tech. Pap. Vol. 37,1443-1446 (2006)

[5] F.L. Pedrotti, L. S. Pedrotti, & L. M. Pedrotti. Introduction to Optics. 3rd ed. Pearson Education Inc. San Francisco, CA. 2007.

[6] E. Hecht. Optics. 3rd ed. Addison Wesley Longman Inc. 1998.

[7] Cowan, Matt. "Presentations (technical)". RealD Media Room downloadable files. 2006.

[8] I. Janossy & L. Szabados. *Optical Reorientation of Nematic Liquid Crystals in the Presence of Photoisomerization*. Physical Review E. Vol 58, No. 4. 4598-4604. (1998)

[9] I. Janossy & L. Szabados. *Photoisomerization of Azo-dyes in Nematic Liquid Crystals*. Journal of Nonlinear Optical Physics and Materials. Vol. 7, No. 4. 539-551. (1998)

[10] D. Statman & I. Janossy. *Study of Photoisomerization of Azo Dyes in Liquid Crystals.* Journal of Chemical Physics. Vol. 118, No. 7. 3222-3232. (2002)

[11] D. Fedorenko, K. Slyusarenko, E. Ouskuva, et al. *Physical Review E* Vol. 77, (2008)

[12] A. Fuh & K. Cheng. *Partially Erasable Photoalignment Layer Formed in Dye-Doped Liquid Crystal Films.* Japanese Journal of Applied Physics. Vol. 45, No. 11, 8778-8781 (2006)

[13] S.T. Wu, Y.S. Chen, J. H. Guo, & A. Y. Fuh. *Fabrication of Twisted Nematic Gratings Using Polarization Hologram Based on Azo-Dye-Doped Liquid Crystals.* Japanese Journal of Applied Physics. Vol. 45, No. 12. 9146-9151. (2006)

[14] W. Y. Wu, T. S. Mo, & A. Y. G. Fuh. *Polarization Characteristics of Diffracted Beams from Twisted Nematic Gratings Fabricated by the Photoalignment Effect in Dye-Doped Liquid-Crystal Films.* J. Opt. Soc. Am. B Vol. 23, No. 9. (2006)

[15] J. C. Chao, W. Y. Wu, & A. Y. G. Fuh. *Diffraction Characteristics of a Liquid Crystal Polarization Grating Analyzed Using the Finite-Difference Time-Domain Method*. Optics Express. Vol. 15, No. 25. (2007)

[16] D. Statman, V. Basore, Y. Sulai, B. Dunlap, and I. Janossy. *Photoinduced Gliding of the Surface Director in Azo-Dye Doped Nematic Liquid Crystals.*

[17]*Polymers and Liquid Crystals.* Case Western Reserve University. 2009

[18]*Electron Microscopy.* ETH Zurich. 2009

[19] Ruslim, C., Komitov, L., Matsuzawa, Y., and Ichimura, K. *Effect of Conformations of Trans- and Cis- Azobenzenes on Photoinduced Anchoring Transitions in a Nematic Liquid Crystal*. Japanese Journal of Applied Physics. Vol. 39, L104-106. (1999)

[20] Malhotra, S.L., Minh, L., Blanchard, L.P. *Thermal Decomposition and Glass Transition Temperature of Poly(ethyl Methacrylate) and Poly(n-butyl Methacrylate).* Journal of Macromolecular Science, Part A, Volume 19, Issue 4 March 1983 , pages 559 - 578

[21] Lee, C.R., Mo, T.S., Cheng, K. T., and Fu, T.L. *Electrically Switchable and Thermally Erasable Biphotonic Holographic Gratings in Dye-Doped Liquid Crystal Cells*. Applied Physics Letters, Vol. 83, No. 21. (2003)

Appendix A - Sample Preparation Procedures

Conventionally, Liquid Crystal Cells are composed of two small rectangular sheets of glass, cut from microscope slides, that sandwich the volume of liquid crystal and are separated by spacers (we use strips of a thin polymer film) of the desired thickness. The cells are glued together and the liquid crystal fills about a 1x1" square within the cell. The procedures for preparing the cells used for our gratings are listed below.

Cleaning Glass Segments

1) Glass slides, cut into 25x25 and 25x35 mm segments, are washed with alconox and deionized (DI) water over a sink.
2) The glass segments are placed in 50 mL beakers (4 in each), side by side, with magnetic stir bars placed between them as spacers.
3) The beakers are filled with DI water, totally submerging the glass segments, and placed in a Branson 2510 sonicator, set for 15 minutes.
4) Without removing the glass segments from the beakers, they are rinsed with DI water 3 times.
5) Repeat 3) with 1M NaOH, followed by 4).
6) Repeat 3) with isopropyl alcohol, followed by 4).
7) Glass segments are dried with N_2 gas.

Preparing Polyimide (PI) solution

1) 2 mL of anhydrous toluene (Sigma-Aldrich) and 8 mL of anhydrous 1-methyl-2-pyrrolidinone (Sigma-Aldrich) are combined.
2) 9 mL of the resulting solution is combined with 3 mL of polyimide (PI-2555) (HD Microsystems).

Preparing Polyethyl-methacrylate (PEMA) solution

0.1 g PEMA (M_w ~515,000 by GPC) (Aldrich) is mixed with 1.8 g toluene (Sigma-Aldrich) to make a 5% (w/w) solution.

Preparing Polyvinyl alcohol (PVA) solution

0.5 g PVA (Aldrich) is mixed with 10 mL DI water and heated to 80°C while stirring until dissolved (1 hr.)

Spin-Coating Polymer Solutions

1) PEMA is to be coated on 25x25 mm glass segments. PI or PVA is to be coated on 25x35 mm glass segments. The clean glass segments are secured on a homemade spin-coating device composed of a pie tin attached to a motor with a variable transformer (Variac) controlling the rotation speed.
2) The polymer is dripped in a Z pattern on the glass.
3) With the motor set at 120 V and the dial set at 30%, the glass is spun for 4 minutes.

Curing PI

1) Immediately after spin-coating, the glass segments are placed in a preheated toaster oven (Black & Decker) at 95°C for 5 minutes.
2) The temperature is increased to 130°C for 5 minutes.
3) The temperature is increased to 150°C for 60 minutes.
4) The temperature is decreased to 130°C for 5 minutes.
5) The temperature is increased to 150°C for 5 minutes.

Curing PEMA

Immediately after spin-coating, the glass segments are placed in a preheated toaster oven (Black & Decker) at 90°C for 60 minutes.

Curing PVA

Immediately after spin-coating, the glass segments are placed in a preheated toaster oven (Black & Decker) at 80°C for 60 minutes.

Aligning PI/PVA-Coated Slides

Rubbing PI or PVA with velvet will cause homogeneous alignment of the liquid crystal (director parallel to the plane of the surface) within the cell. A homemade device with two parallel rails running under a secured piece of velvet allows one to move glass segments along the rails to contact the velvet in the same way multiple times. This is done 5 times.

Binding Cells

1) Two thin strips of polymer film are used as spacers for each cell (polyimide film, 7.5 µm thick; from Chemplex). They are cut from a roll with scissors.
2) The spacers are sandwiched between the polymer sides of a 25x35 mm segment and a 25x25 mm segment of glass, with the spacers along opposite edges. These two edged are then sealed with epoxy.
3) Cells are left under pressure using clips for at least 24 hours.

Doping Liquid Crystals

This is simply done by weighing out the proper amount of azo dye and adding it to the liquid crystal in a vial, for 0.5% (w/w). Typically, a few hundred milligrams of liquid crystal can make dozens of samples, so it is useful to weigh out the dye on a scale which is accurate to fractions of a milligram. The mixture is mixed in the sonicator until well blended.

Filling Cells

Cells are filled dropwise along an unsealed edge, allowing the cell to fill by capillary action. Any excess is wiped off. Unsealed edges are then sealed with epoxy.

Flaws in Sample Preparation Procedure

Two problems were encountered after preparing cells according to the procedure above: cell spacing is non-uniform, and cell spacing was much larger than the thickness of the spacers. Measurements of the cell spacing showed different results in different areas of cells, with pressure points apparent to the naked eye. This is because the pressure placed on the cell while the glue dries, is not uniform because the spacers are only on the edges. An examination of high quality premade cells from AlphaMicron shows that microspheres are distributed all throughout their cells, to ensure uniform spacing. These microspheres are nonreactive, and spaced far enough with respect to the liquid crystal molecules that they do not affect the results. It should be inexpensive to acquire the microspheres for use in the future.

The cells are also not as thin as desired; being much thicker because of the use of a quick-dry epoxy, which expands slightly as it dries. A non-expansive permanent adhesive should remedy this problem. Due to the problems encountered with the spacing of my cells, no conclusions can be drawn relating any of the results to the cell spacing.

Perhaps the biggest flaw in my samples would be that they are not rewritable. It was unforeseen that the gratings could not be erased with light, and that the use of PEMA in my samples would prevent a thermally induced erasure from working. Although using a different polymer aside from PEMA could allow one to thermally erase samples, several controlled heating and cooling cycles may take more time than one would be willing to spend on erasing a sample, and we would only be putting off an analysis of samples using PEMA. Perhaps a more fruitful idea would be to consider a new photoalignment method, which would also be useful for setting an initial orientation on the polymer surface without contact, as opposed to rubbing with felt and risking contamination with dust.

Appendix B - Measurement of Empty Cells

Using an Ocean Optics Spectrometer, one may measure the spacing of empty cells because the interference pattern within the cell is dependent on the spacing of the cell, so the spacing can be determined by:

$$d = \frac{\lambda_1 \lambda_2}{2\Delta\lambda} \qquad (11)$$

Where d is the spacing, λ_1 and λ_2 are the wavelengths of any two adjacent transmission peaks, and $\Delta\lambda$ is the difference in wavelength between those peaks.

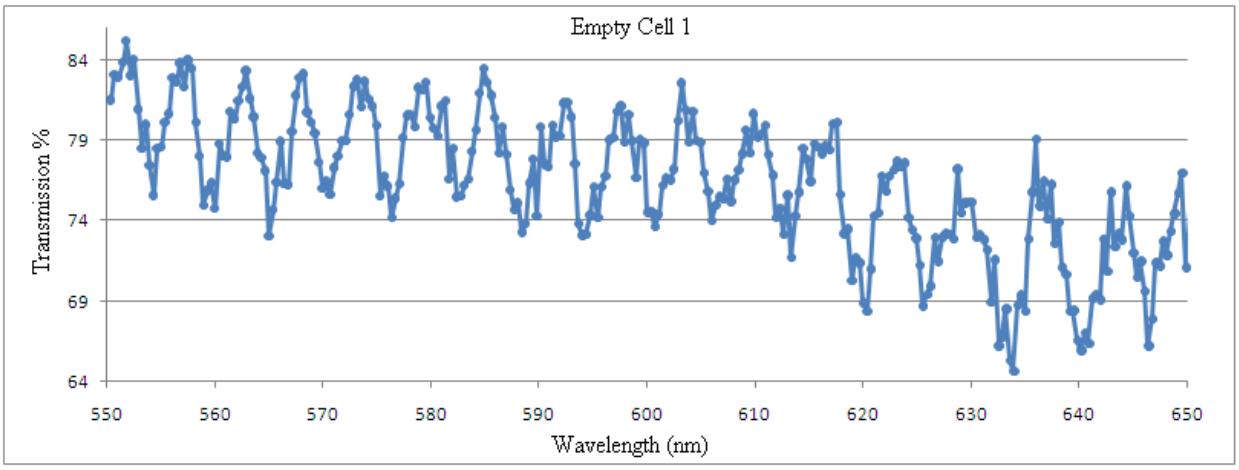

Fig. 13: Spectrum from an empty cell. Since d is constant, peaks get further apart as wavelength increases. The spacing in this cell is about 28.5 µm.

Derivation of Eqn. [11]

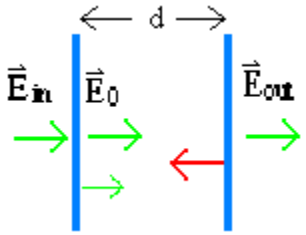

Fig. 14: Measurement of an empty cell. The blue vertical lines represent plates of glass that make up the cell. $\vec{E}_{in}$ is the wave coming from the source, $\vec{E}_0$ is the wave within the cell, traveling towards the detector, and $\vec{E}_{out}$ is the wave reaching the detector, out the other side of the cell. The red arrow represents waves being reflected by the glass plate on the right. The cell spacing is d.

We seem to define $\vec{E}_0$ as the wave transmitted after $\vec{E}_{\text{in}}$ contacts the glass plate on the left, but we also consider that waves which reflect from the glass plate on the right and reflect once more from the glass plate on the left, ending up in the same direction as $\vec{E}_0$, also contribute to the overall wave within the cell. Thus, $\vec{E}_0$ is defined as:

$$\vec{E}_0 = t\vec{E}_{in} + r^2\vec{E}_0 e^{ik2d} \quad (12)$$

Where t is the transmission coefficient, r is the reflection coefficient, and $k = 2\pi/\lambda$.

Simplified:

$$\vec{E}_0 = \frac{t\vec{E}_{in}}{1-r^2 e^{ik2d}} \quad (13)$$

We can then write:

$$\vec{E}_{out} = t\vec{E}_0 e^{ikd} \quad (14)$$

$$\frac{\vec{E}_{out}}{\vec{E}_{in}} = \frac{t^2 e^{ikd}}{1-r^2 e^{ik2d}} \quad (15)$$

Multiplying Eqn. 7 by the complex conjugate yields:

$$\frac{I_{out}}{I_{in}} = \frac{t^2}{(1-r^2 e^{ik2d})(1-r^2 e^{-ik2d})} \quad (16)$$

Where I_{out} is the irradiance out and I_{in} is the irradiance in. In this case, we can simplify further by using Euler's Identity, and noting that T, the transmittance, is t^2, and R, the reflectance, is r^2:

$$\frac{I_{out}}{I_{in}} = \frac{T}{1+R^2-2Rcos(2kd)} \quad (17)$$

At this point, it becomes apparent that the distance between two peaks on the spectrum, which is every 2π radians, obeys the following relation:

$$2\pi = 2kd = \frac{4\pi d}{\lambda} \quad (18)$$

and that for two adjacent peaks at λ_1 and λ_2:

$$2\pi = \frac{4\pi d}{\lambda_2 - \lambda_1} \quad (19)$$

Solving for *d* yields (11).

Using this calculation would only serve as a rough estimate. A spreadsheet calculation is used to essentially average this estimate over many peaks.

Appendix C - Mathematical Representation of Polarization

Jones Vectors are mathematical representations of polarized light. Jones Matrices represent changes in polarization, by polarizing elements. Since the state of polarization is completely determined by relative amplitude and phase components, Jones Vectors and Jones Matrices are useful when we are only concerned with transformations of polarization.

To keep things simple, we can define a Cartesian coordinate system such that whichever direction the laser beam propagates will be the z-direction. By this system, relevant components are kept in the x,y-plane.

The Jones Vector representation is written as:

$$\tilde{E}_0 = \begin{bmatrix} E_{0x} e^{i\varphi_x} \\ E_{0y} e^{i\varphi_y} \end{bmatrix} \tag{20}$$

Where $\tilde{E}_0$ is the complex amplitude vector, with amplitudes E_{0x} and E_{0y}, and phases φ_x and φ_y.

For greater simplicity, we employ a normalization condition such that for a vector $\begin{bmatrix} a \\ b \end{bmatrix}$, it is expressed in its normalized form when:

$$|a|^2 + |b|^2 = 1 \tag{21}$$

Linear polarizations set at some angle α from the x-axis can be written as:

$$\tilde{E}_0 = \begin{bmatrix} cos\ \alpha \\ sin\ \alpha \end{bmatrix} \tag{22}$$

Linear polarizations have a phase difference of 0 or π, circular polarizations are at π/2 or 3π/2, and all other phase differences produce an elliptical polarization. The normalized forms of the left-circularly polarized and right-circularly polarized light needed to create the interference pattern desired to make polarization gratings are:

$$\tilde{E}_0 = \frac{1}{\sqrt{2}} \begin{bmatrix} 1 \\ i \end{bmatrix} \quad LCP \qquad \tilde{E}_0 = \frac{1}{\sqrt{2}} \begin{bmatrix} 1 \\ -i \end{bmatrix} \quad RCP$$

The addition of the two vectors yields:

$$\tilde{E}_0 = \frac{1}{\sqrt{2}}\begin{bmatrix}2\\0\end{bmatrix}$$

In other words, interference of the two beams yields linear polarization of twice the original amplitude.

Jones Matrices are matrices which represent transformations in polarization. If you know the Jones Vector you desire and the Jones Vector you start with, you can derive the appropriate Jones Matrix. The main polarizing elements of interest in my setup are a quarter-wave plate and a beam splitter. Light coming from the Ar^+ laser is horizontally polarized. When it passes through the quarter-wave plate with the fast-axis of the wave plate aligned 45° or -45° to the polarization of the beam, a circular polarization is produced. As an example, consider a beam of light polarized at angle 45° transmitted through a quarter-wave plate with a vertical fast axis:

$e^{i\pi/4}\begin{bmatrix}1 & 0\\0 & -i\end{bmatrix}$	QWP, vertical FA	
$\frac{1}{\sqrt{2}}\begin{bmatrix}1\\1\end{bmatrix}$	Linear, at 45°	
$e^{i\pi/4}\begin{bmatrix}1 & 0\\0 & -i\end{bmatrix}\frac{1}{\sqrt{2}}\begin{bmatrix}1\\1\end{bmatrix} = e^{i\pi/4}\frac{1}{\sqrt{2}}\begin{bmatrix}1\\-i\end{bmatrix}$	Right-circular polarization	(23)

Although the Jones Vectors are a handy way of describing the polarization of light, as described in Appendix C, they can only be used for totally polarized light. Experimentally, we measure the Stokes Parameters because they are applicable to unpolarized and partially polarized light as well. The operational definition of the Stokes Parameters is given by:

$$\mathcal{S}_0 = 2I_0 \qquad (24\text{ a})$$

$$\mathcal{S}_1 = 2I_1 - 2I_0 \qquad (24\text{ b})$$

$$\mathcal{S}_2 = 2I_2 - 2I_0 \qquad (24\text{c})$$

$$\mathcal{S}_3 = 2I_3 - 2I_0 \qquad (24\text{ d})$$

Where $\mathcal{S}_0$ is simply the incident irradiance, and the other 3 parameters specify the state of polarization. I_1 and I_2 are the transmitted irradiances after being filtered through a linear polarizer set at the horizontal and at +45°, respectively. I_3 is the transmitted irradiance through a filter which only allows right-circular polarization to pass. It is often handy to normalize the Stokes Parameters by dividing each one by the value of $\mathcal{S}_0$. For completely polarized light,

$$\mathcal{S}_0{}^2 = \mathcal{S}_1{}^2 + \mathcal{S}_2{}^2 + \mathcal{S}_3{}^2 \tag{25}$$

The degree of polarization V, is a measure of how well polarized a beam of light is. The general expression is:

$$V = \frac{I_{max} - I_{min}}{I_{max} + I_{min}} \tag{26}$$

Where I_{max} and I_{min} are the values one would observe if one were to rotate a linear polarizer in front of the beam.

One can see that for perfectly linear light, I_{min} would be zero, and $V = 1$. For unpolarized or circularly polarized light, $I_{max} = I_{min}$, so $V = 0$. Using the Stokes Parameters, it can be shown that:

$$V = \left(\mathcal{S}_1{}^2 + \mathcal{S}_2{}^2 + \mathcal{S}_3{}^2\right)^{1/2} / \mathcal{S}_0 \tag{27}$$

Notice from (25) that if the light is perfectly polarized, $V = 1$, inclusive of the case of circularly polarized light, and that $V = 0$ for only unpolarized light.